DOI: 10.1002/cbic.200800326

Supramolecular Domains in Mixed Peptide Self-Assembled Monolayers on Gold Nanoparticles

Laurence Duchesne,[a] Geoff Wells,[b] David G. Fernig,[a] Sarah A. Harris,[c] and Raphaël Lévy*[a]

Self-organization in mixed self-assembled monolayers of small molecules provides a route towards nanoparticles with complex molecular structures. Inspired by structural biology, a strategy based on chemical cross-linking is introduced to probe proximity between functional peptides embedded in a mixed self-assembled monolayer at the surface of a nanoparticle. The physical basis of the proximity measurement is a transition from intramolecular to intermolecular cross-linking as the functional peptides get closer. Experimental investigations of a binary peptide self-assembled monolayer show that this transition happens at an extremely low molar ratio of the functional versus matrix peptide. Molecular dynamics simulations of the peptide self-assembled monolayer are used to calculate the volume explored by the reactive groups. Comparison of the experimental results with a probabilistic model demonstrates that the peptides are not randomly distributed at the surface of the nanoparticle, but rather self-organize into supramolecular domains.

Introduction

Inspired by highly elaborated multi-unit nanomachines observed in biological systems, molecular self-assembly was proposed over 15 years ago as a general route for the synthesis of functional nanostructures.[1] Since then a large variety of structures have been produced;[2] some of the most remarkable examples use DNA itself as a structural building block.[3,4] However, the challenge set by Whitesides and collaborators of making "structures of the size and complexity of biological structures" is still current[1] and a significant part of this challenge resides in the elucidation with subnanomolecular resolution of the complex structures that are formed through self-assembly. Structural biology, that is, the determination of the three-dimensional shape of biomolecules, has revealed how biological nanomachines work on the atomic scale. Chemical cross-linking, by virtue of identifying the proximity between key chemical groups, has made critical contributions to this field.[5] Structural nanotechnology, that is, the determination of the structures of nanomaterials at the submolecular scale, is essential for the future production of artificial nanomachines.[6]

Self-assembled monolayers (SAMs) of thiolated small molecules provide a convenient way of controlling the surface properties of metal nanoparticles[7,8] leading in some cases to protein-like properties, for example, specific recognition, enzyme inhibition or catalytic activity.[9–11] Studies on planar SAMs suggest that domains could be engineered through phase separation, which generally occurs in mixed SAMs[12,13] and has also been observed in mixed self-assembled peptide nanofibers.[14] Such phase separation is similar to the formation of domains in mixed lipid monolayers and phospholipid membranes.[15,16] Scanning tunneling microscopy (STM) studies on gold nanoparticles have revealed pattern formation in mixed SAMs of alkane thiolates.[17,18] An X-ray study of bifunctional gold nanoparticles at the air-water interface suggests the formation of giant amphiphiles through segregation of hydrophobic and hydrophilic ligands.[19,20] In another study, nanoparticles were prepared with mixed SAMs composed of ligands which had been designed to phase-separate, and a blue shift of the surface plasmon band was observed and interpreted as indicating the formation of Janus nanoparticles.[21] Control over the formation of heterogeneities in mixed SAMs on nanoparticles would allow the design of nanoparticles with well-defined complex surfaces, opening new possibilities for catalysis and bottom-up assembly of nanodevices.[9,17,22–26] Acquiring such control requires the means to interrogate the SAM molecular structures with a high degree of chemical specificity and a high throughput. To this end, we have designed a proximity probe based on chemical cross-linking, which, in conjunction with molecular dynamics simulations, reveals self-organization in a mixed peptide SAMs on gold nanoparticles.

The formation of peptide SAMs on gold nanoparticles provides a simple approach to generate nanomaterials with a high degree of chemical complexity.[8,27] The complexity can be encoded through the design of peptide sequences and through the combination of different peptides on a single

[a] *Dr. L. Duchesne, Prof. D. G. Fernig, Dr. R. Lévy*
School of Biological Sciences and Liverpool Institute of Nanoscale Science Engineering and Technology, University of Liverpool
Biosciences Building, Crown Street, Liverpool L69 7ZB (UK)
Fax: (+44) 151-795-4406
E-mail: rapha@liverpool.ac.uk

[b] *Dr. G. Wells*
Department of Pharmaceutical and Biological Chemistry
The School of Pharmacy, University of London
29–39 Brunswick Square, London, WC1N 1AX (UK)

[c] *Dr. S. A. Harris*
School of Physics and Astronomy, University of Leeds
Leeds LS2 9JT (UK)

Supporting information for this article is available on the WWW under http://www.chembiochem.org or from the author.

nanoparticle. To evaluate whether the different peptides are randomly distributed or if they self-organize to form supramolecular domains, peptide-capped gold nanoparticles (10 nm diameter) covered with a binary peptide SAM composed of a matrix peptide and of a longer functional peptide were prepared. Molecular cross-linking was used to measure the proximity between the functional peptides for various SAM compositions. Each functional peptide contains two reactive groups that can be chemically cross-linked together (intramolecular cross-linking) or with a reactive group on another functional peptide (intermolecular cross-linking). If a given functional peptide is isolated from other functional peptides, it will form an intramolecular bond upon addition of the cross-linker, whereas if there is another functional peptide in close proximity, intermolecular cross-linking can occur (Figure 1). The transition between the formations of intra- versus intermolecular cross-links defines a critical separation (sepcrit) and provides the physical basis of a proximity measurement (Figure 1).

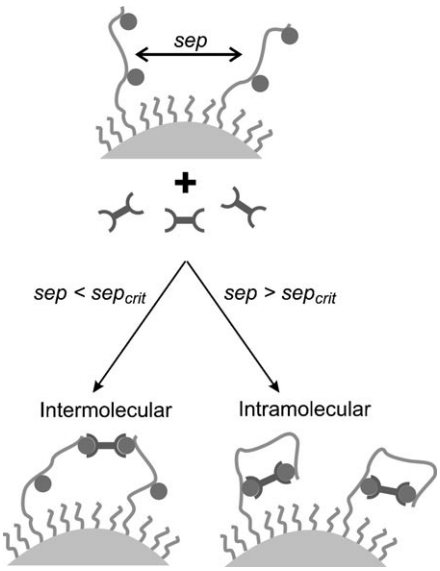

Figure 1. A proximity probe based on the transition between inter- and intramolecular cross-linking. The circles represent reactive groups that can be cross-linked by the homobifunctional cross-linker. "sep" is the separation between the functional peptides. sepcrit is the separation at which the transition from intra- to intermolecular cross-linking occurs.

Results and Discussion

Competition between intra- and intermolecular bond formation

The measurement principle, that is, competition between intra- and intermolecular bond formation, ensures rapid completion of the cross-linking reaction: once one of the active groups of the cross-linker has reacted, the other active group is constrained in a space where at least one other reactive group is available for reaction resulting in a very high local concentration of reactant. This prevents interparticle cross-linking, which would otherwise induce nanoparticle aggregation.[28,29] UV–visible absorbance spectra after cross-linking do not exhibit any plasmon band shift, confirming the absence of aggregation (see Figure S1 in the Supporting Information).

Formation of peptide loops

In order to demonstrate that chemical cross-linking can be used to form intramolecular bonds (loops), a reporter system was coded into the sequence design of the functional peptide (Figure 2A). The loop is obtained by cross-linking the two primary amines on the 7th and 20th amino acid (lysine residues) of the functional peptide using the homobifuntional cross-linker bis(sulfosuccinimidyl)suberate (BS3). The peptide N-terminal amino group on the cysteine is in contact with the gold surface and, therefore, not accessible for reaction.[27] The sequence between the two lysines in positions seven and 20 contains the cleavage site of the protease thrombin (positions 10–15) and a biotinylated lysine in position 17 (note that the biotinylated lysine does not have a primary amine). The effect of thrombin and BS3 on a single functional peptide is schematically shown in Figure 2B. Thrombin cleavage will result in the loss of the biotin on the linear peptide but not on the loop. The presence of the biotin on the nanoparticle after cross-linking and cleavage is, therefore, a signature of the successful closure of the loop.

To vary the average distance between functional peptides, nanoparticles coated with SAMs of different composition were prepared. The peptide solutions used to form the SAM contained 0.08, 0.24, 0.72 and 2.1% (mol/mol) of the functional peptide (Figure 2A) and a balance of matrix peptide (CALNN). The corresponding molar composition of the monolayer was measured as described in ref. [30]. Briefly, nanoparticles having one or more functional peptides (so carrying one or more biotins) can be pulled down with streptavidin affinity beads. For a given molar ratio of functional peptide, the proportion of nanoparticles pulled down is a direct measurement of the proportion of nanoparticles having one or more functional peptide.[30] Quantitative analysis of the pull-down experiment (Figure 3) indicates that the average number of functional peptide per nanoparticle $N_{average}$ is equal to 1, 2.9, 8.8, or 26 functional peptides per nanoparticle for the solutions containing 0.08, 0.24, 0.72, or 2.1% of functional peptide, respectively.[30] The first column in Figure 2C confirms that the biotin can be detected for the different SAM compositions. However, after incubation with thrombin, biotin is no longer detected on the nanoparticles (Figure 2C, column 2). This constitutes another example of how natural enzymes can be used to manipulate the chemical state of nanoparticles.[31–35] When the nanoparticles have been exposed to the cross-linker (Figure 2C, columns 3 and 4), thrombin activity does not result in the loss of biotin indicating that BS3 has successfully cross-linked functional peptides at the surface of the nanoparticles.[36]

Transition from intra- to intermolecular loops

To examine whether intermolecular cross-linking occurs, the oligomerization state of the cross-linked functional peptides

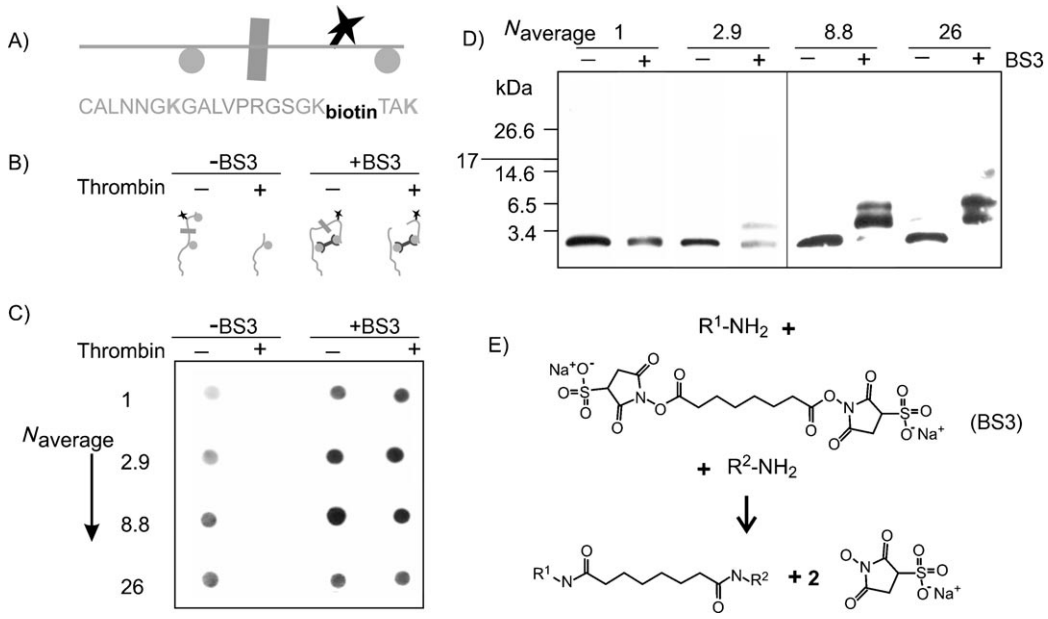

Figure 2. A) Functional peptide. The circles represent the amino group that can react with BS3. The rectangle represents the thrombin cleavage site. The star represents a biotin. B) Illustration of the effect of the homobifunctional cross-linker BS3 and thrombin on a single functional peptide. C) Presence of biotin detected by chemiluminescence (Dot-blot) on peptide-capped gold nanoparticles with/without BS3 treatment and exposed or not to thrombin. D) Western-blot of functional peptides from nanoparticles that have been treated (or not) with BS3. The experiments were performed with nanoparticles having different average number of functional peptides per nanoparticle ($N_{average} = 1$, 2.9, 8.8, 26). E) Cross-linking reaction.

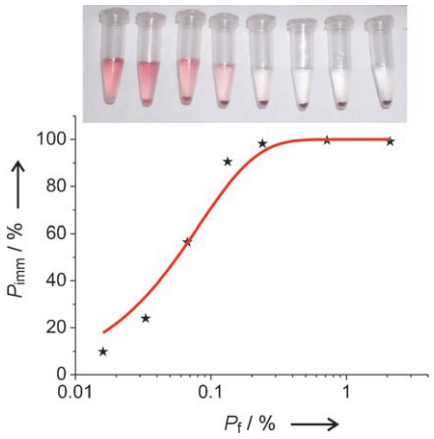

Figure 3. Proportion of biotinylated NPs as a function of the proportion of functional versus matrix peptides in the nanoparticle preparation. Peptide-capped nanoparticles were prepared with different proportion of functional peptide (P_f). P_{imm} is the percentage of biotinylated nanoparticles as measured by the proportion of nanoparticles pulled-down by streptavidin–agarose beads. Inset: visual illustration of the experiment showing the binding of the nanoparticle to the streptavidin–agarose beads (pellet).

were analyzed by Western-blot. Short peptide fragments are normally difficult to detect because they pass through the membrane during the electrotransfer step and because of their weak binding to the membrane. Therefore, a modified Western-blotting procedure with gold and silver-coated membranes to immobilize the peptides was used.[37] For $N_{average} = 1$, with or without cross-linker, only a single band can be seen and its molecular weight corresponds to that of the monomer (2.2 kDa). Taken together with the results shown in Figure 2C, this demonstrates the formation of intramolecular loops, which have the same molecular weight as the untreated monomer (Figure 2D), but retains biotin upon thrombin treatment (Figure 2C). This is not surprising, since, for $N_{average} = 1$, a large proportion of the nanoparticles have a single functional peptide at their surface. For higher values of $N_{average}$, the monomer band disappears and higher M_W bands appear, indicating the formation of oligomeric species through intermolecular cross-linking (Figure 2D). This is further confirmed by mass spectrometry analysis of the fragments released from the cleavage experiments (Figures S2–S4). The transition from intra- to intermolecular cross-linking is already visible for $N_{average} = 2.9$ for which both a monomer and a dimer band can be seen. For $N_{average} = 8.8$ and 26, the intensity of the monomer band becomes negligible and oligomers larger than dimers are formed.

Distances explored by reactive groups

On planar surfaces, it is generally agreed that reactive sites are isolated from one another in SAMs in which less than 1% of the molecules are reactive.[7] In our experiments, the monolayers were prepared from peptide mixtures containing only 0.08, 0.24, 0.72, or 2.1% of the functional peptide, resulting in low grafting densities of one functional peptide for 347, 115, 38, or 13 nm^2. These results suggest that the functional peptides are clustered prior to the addition of the cross-linker. To test this hypothesis, a model was built to predict the intensity of the first band (monomer) after cross-linking if the functional molecules were randomly dispersed. A minimum value of the intensity can be calculated from the fraction of functional peptide that cannot undergo intermolecular cross-linking, because they

do not have a neighbouring functional peptide at a separation below sepcrit. In order to estimate sepcrit, molecular dynamics (MD) simulations of the functional peptide were used to quantify the distances explored by the reactive amine on Lys20. MD simulations were also performed for the functional peptide after reaction of one of the *N*-hydroxysuccinimide (NHS) ester of the BS3 on the Lys20. First, we performed a MD simulation in which the entire nanoparticle peptide SAM is represented atomistically, including two functional peptides, one of which has been reacted with BS3 (See Figure S5 in the Supporting Information). The attachment of the peptides to the gold surface is mimicked by fixing the positions of the N-terminal cysteine residues. The peptides all start from an elongated configuration, but undergo entropic collapse to a more compact state as the simulation proceeds (see Movie S1 in the Supporting Information).

Based on this preliminary simulation, a reduced representation of the system was constructed to decrease the computational cost of quantifying the volume explored by a functional peptide chain. A pair of curved surfaces made of 11 by 11 peptides was constructed with the matrix peptides held fixed at a separation of 8 Å and represented only by the C-terminal asparagine of the matrix peptide with an N-terminal acetyl group (Figures 4A and B and Figure S6). The functionalized peptides with and without the BS3 linker are placed in the centre of each surface. To calculate the volume of space explored, a simulated annealing protocol in which the peptides are systematically heated and then cooled prior to data collection was used to improve exploration of conformational space. No persistent secondary structural elements were detected during the simulations. A representative molecular configuration for each peptide is shown in Figure 4C and D, the distribution of distances explored by the functional groups are shown in Figures 4E and F, and movies of the simulation trajectories are provided (See Movies S2 and S3 in the Supporting Information).

Functional peptide interaction with the SAM

The functional peptides interact strongly with the SAM. In the absence of BS3, this leads to a bimodal distribution of the vertical distance between the primary amine group of Lys20 and the gold surface (Figure 4E, red curve). The first sharp peak at 12 Å corresponds to the lysine being in contact with the matrix peptide surface while the second broader peak corresponds to the lysine moving above the surface (Movie S2). When the amino group has been reacted with BS3, the distribution of vertical distances becomes unimodal (Figure 4F, red curve, and Movie S3). This can be understood by looking at the electrostatic potential maps for the functional peptide with and without BS3 (Figure 5). Because of the carboxylic acid terminus of CALNN, the SAM surface is negatively charged,[27] whilst the lysine and arginine residues within the functional peptide sequences give rise to positive electrostatic potential. These positively charged regions strongly attract the peptide to the surface, which explains the first peak in the bimodal distribution of Figure 4E.

The BS3 derivatized lysine is negatively charged removing favourable electrostatic interactions with the SAM. Consequently, the conformations of the functional peptides are less

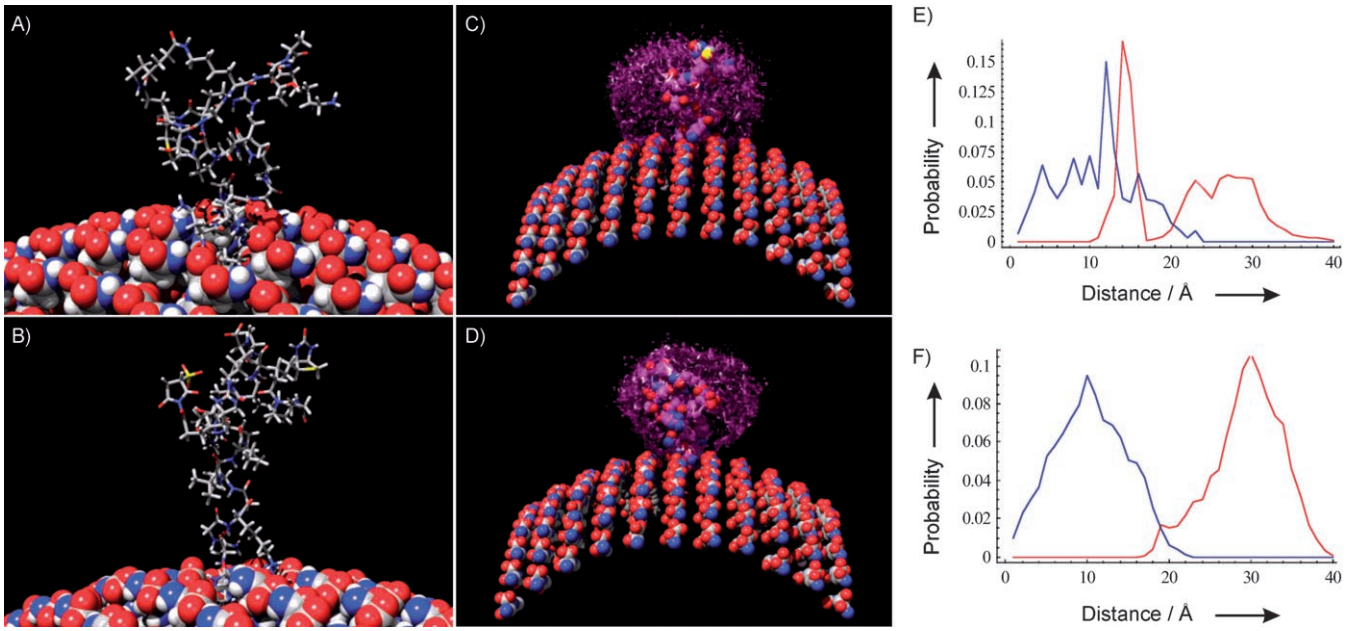

Figure 4. Molecular configurations taken from the MD simulation of the functionalized peptides: functional peptide (A); functional peptide with BS3 reacted on Lys20 (B); the volume of conformational space explored by the functionalized peptides is shown superimposed on a representative configuration without (C) and with (D) the BS3 linker; the distribution of horizontal (blue) and vertical (red) distances explored by the reactive group on the functional peptide (E) and on the functional peptide with BS3 reacted on Lys20 (F). The distributions were measured from the MD trajectories. The distance measurements are from the sulfur atom on the N-terminal cysteine residue to either the side-chain nitrogen on Lys20 (functional peptide) or to the carbon atom of the activated ester on the BS3 linker (functional peptide with BS3 reacted on Lys20).

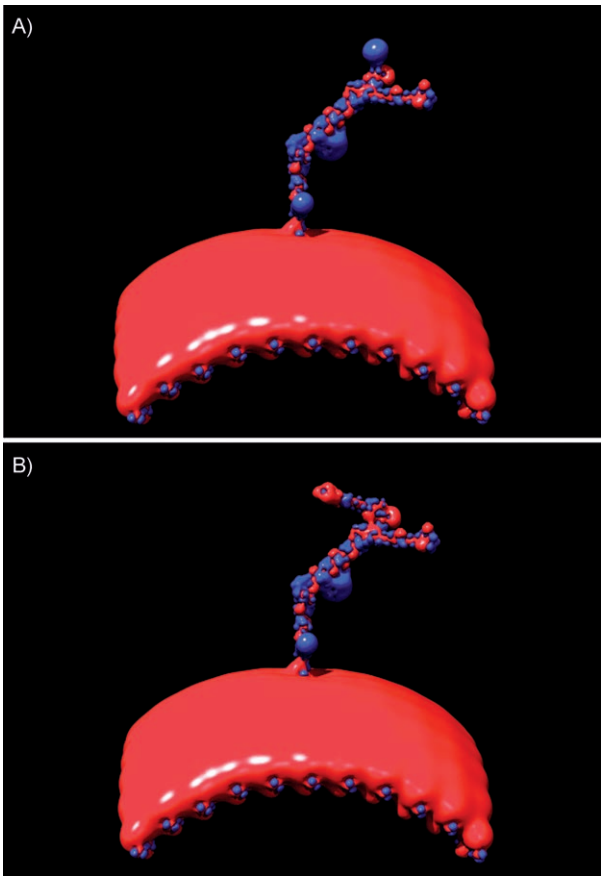

Figure 5. Electrostatic potential maps calculated for functionalized peptides without (A) and with (B) the BS3 linker. Red indicates a negative potential of −2, the surface of positive potential of +0.5 is shown in blue. The units of potential are kTe^{-1}. The peptides are shown in elongated configurations for clarity.

compact when the linker is attached, and the vertical displacements of the reactive carbon atom from the attachment point are unimodal. This change in shape of the explored volume leads to the unexpected result that the presence of the 11.4 Å spacer arm of the BS3 does not lead to an increase in the distances explored across the surface. Both the primary amine on the unreacted lysine of the functional peptide and the reactive NHS ester on the attached BS3 are constrained within ~20 Å of the attachment point of the functional peptide (Figures 4E and F, blue curves). While the relative rates of formation of intra- versus intermolecular cross-linking certainly depend on the distance between two peptides, formation of intermolecular cross-linking is only possible if there is some overlap between the volumes explored by the two reacting groups. Therefore, from the MD simulations, we can conclude that the rate of formation of intermolecular cross-links is zero for functional peptides which are separated by more than 40 Å.

Nonrandom localization of functional peptides

Assuming a Poisson distribution of the number of functional peptides per nanoparticle and a random localization of the peptides at the surface of the nanoparticle, the probability for a given functional peptide to have no neighbouring functional peptide closer than 40 Å was calculated (see the Supporting Information). If the functional peptides were to be randomly distributed, for $N_{average}=1$, 2.9, 8.8, or 26, this simple model predicts that respectively 94, 83, 57, or 19% of the functional peptide would have no neighbouring peptides within 40 Å and, therefore, would not be able to participate in intermolecular cross-linking. These probabilities provide a minimum value for the intensity of the monomer band in Figure 2D that would be observed if the functional peptides were randomly distributed. Clearly the experimental results are not compatible with a random localization of the functional peptides (Figure 2D) but rather indicate that the functional peptides self-organize. The disappearance of the monomer band could be explained by the formation of several dimeric species or by the formation of larger patches or supramolecular domains. The appearance for $N_{average}=8.8$ and 26 of bands corresponding to larger oligomers (Figure 2D) indicate that the second interpretation is correct and that supramolecular domains composed of more than two functional peptides in close proximity are formed.

To examine whether clustering of the functional peptide occurs in solution before the formation of the monolayer, a cross-linking experiment was performed in conditions identical to those used for the preparation of the nanoparticles but in the absence of nanoparticles. In contrast with the results obtained with the peptide-capped nanoparticles, the functional peptide was found to be in its monomeric form (Figure S7). At concentrations of functional peptides five times higher than those used in the nanoparticle experiments, the formation of dimers was observed but no higher molecular weight oligomers were observed even at the highest concentration tested (Figure S7). These results clearly demonstrate that the self-organization occurs during the formation or maturation of the self-assembled monolayer.

In order to obtain insights into the mechanisms of self-organization, the dynamics of the formation of the supramolecular domains was probed for $N_{average}=8.8$. Remarkably, the monomer band disappears within the first few minutes of the formation of the monolayer (Figure 6) and the first oligomer

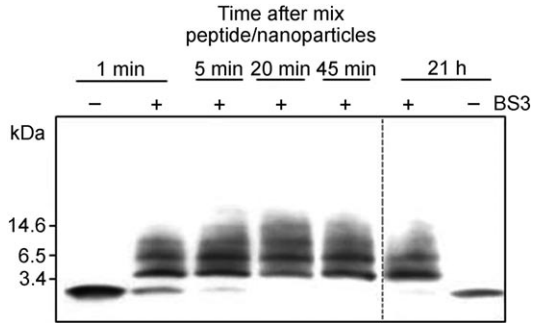

Figure 6. Western-blot of functional peptides from nanoparticles that have been treated (or not) with BS3 as a function of the peptide–nanoparticle reaction time (1, 5, 30, 45 min and 21 h after mixing the peptide and the nanoparticle solutions). The experiments were realized with a peptide solution containing 0.72% functional peptide (corresponding to nanoparticles having an average of 8.8 functional peptides per nanoparticle).

bands can already be seen even after 1 min;[38] note that the time value refers to the addition of the cross-linker and that the cross-linking reaction is expected to be complete within 2 min in the experimental conditions used.[39,40] These rapid dynamics seem more compatible with a mechanism in which the formation of the domain results from local enrichment in functional peptide through preferential adsorption followed by ligand exchange rather than by a mechanism of random diffusion of the functional peptides within the SAM.

Conclusions

Nanotechnology scientists face a challenge similar to the one faced by structural biologists half a century ago: determining with atomic-scale precision the structure of a whole range of nanoparticle/proteins. This article introduces a new approach for investigating the molecular structures of mixed monolayers at the surface of nanoparticles. While further experimental and theoretical work will be required to understand and predict self-organization in mixed peptide SAMs, this work opens a route towards the design and synthesis of nanoparticles that have complex surfaces composed of several functional supramolecular domains.

Experimental Section

Materials: The peptides CALNN (also referred to as matrix peptide) and CALNNGKGALVPRGSGKbiotinTAK (also referred to as functional peptide) were purchased from Sigma-Genosys Ltd (Haverhill, UK). The 10 nm gold nanoparticles (G-NPs) were purchased from British Biocell (BBInternational Ltd, UK). Sephadex G25 superfine, Bovine serum albumin, Tween 20, streptavidin–agarose and thrombin protease (3.4.21.5) were purchased from Sigma–Aldrich Ltd (Dorset, UK). Bis[sulfosuccinimidyl]suberate (BS3) and SuperSignal West Pico Chemiluminescent Substrate were purchased from Pierce (Perbio Science UK Ltd). Immobilon-P polyvinylidene difluoride (PVDF) membranes were purchased from Millipore (Watford, UK). Strep-Tactin-HRP (horse radish peroxidase) was purchased from IBA (Göttingen, Germany). Nanosep centrifugal units were from PALL (PALL Corp., Portsmouth, Hants, UK). Polypeptide SDS-PAGE standards were purchased from Biorad (BioRad, Hemel Hempstead, UK).

Preparation of peptide-capped gold nanoparticles: In the following, PBS is meant for Phosphate Buffer Saline (Na_2HPO_4 (8.1 mM), KH_2PO_4 (1.2 mM), NaCl (150 mM) and KCl (2.7 mM), pH 7.4) and 10×PBS for 10 times more concentrated solution of the same salts. The peptide stock solutions were prepared by dissolving the peptide powders in 10×PBS and then aliquoted and kept at −80 °C until further use. Before use, the matrix peptide and the functional peptide (2 mM final concentration) were mixed into the desired molar ratio, and gold solution was added to this peptide solution in a 10:1 volume ratio. The reaction was left overnight at 4 °C, and the excess peptide was then removed by size-exclusion chromatography with Sephadex G25 superfine as separation medium and PBS as the mobile phase (except for the time-dependence experiments of Figure 6, see below).

UV/Vis spectrometry: Absorption spectra were recorded at room temperature using a Spectra Max Plus spectrophotometer (Molecular Devices, Wokingham, UK).

Number of functional peptides per gold nanoparticle: Peptide-capped nanoparticles with different ratios of matrix/functional peptides were prepared (8 nM nanoparticle concentration in PBS). The nanoparticle solution (200 μL) was added to streptavidin–agarose beads (10 μL) equilibrated in PBS. The reaction was incubated overnight at room temperature under agitation. The beads were then left to sediment and the amount of unbound nanoparticles was quantified by the measurement of the absorbance at 520 nm of the supernatant.

Cross-linking on peptide-capped nanoparticles (Figure 2): Concentration of peptide-capped nanoparticles were adjusted to 5 nM with PBS. Cross-linking was performed by adding bis[sulfosuccinimidyl]suberate (BS3) to a 10 mM final concentration. Cross-linking on nanoparticles bearing a different ratio of loop/matrix peptides was performed for 2 h at room temperature, and the reaction was stopped by addition of Tris-HCl (pH 8) to a 10 mM final concentration.

Cross-linking on peptide-capped nanoparticles (Figure 6, time dependence): For each ratio of peptide-capped nanoparticles, the sample was divided into two, one was treated with BS3 (10 mM) and the other mocked treated. Cross-linking performed at different time points during the matrix self-assembly was performed by adding the cross-linker at given times (1, 5, 30, 45 min, 21 h) after the mix between nanoparticles and peptides. The reaction was stopped after 5 min (1, 5, 30, 45 min time points) or 40 min by addition of Tris-HCl pH 8 (10 mM final concentration). Excess of BS3 and Tris-HCl was removed using nanosep centrifugal devices (cut-off 30 K).

Thrombin protease digestion: Peptide-capped nanoparticles in PBS, treated or untreated with BS3, were adjusted to 5 nM concentration. Each sample was divided into two, one was treated with thrombin and the other mocked treated. Thrombin digestion was performed by adding the protease (25 mU) and NaCl (250 mM final concentration). The mixture was left incubated overnight at 37 °C and the digestion reaction was repeated two further times (25 mU, then 50 mU, 3 h incubation times at 37 °C). The reaction mixture was then centrifuged for 45 min (15 000 *g* at 4 °C). The supernatant (thrombin enzyme and cleaved material from peptide-capped nanoparticles) was loaded onto a nanosep centrifugal device and the flow-through (cleaved material) was freeze-dried for further analysis. The pellet (peptide-capped nanoparticles) was resuspended in PBS (1 mL) and washed again by four cycles of centrifugation (45 min, 15 000 *g*, 4 °C).

Dot- and Western-blotting: After BS3 and thrombin treatment, the concentration of peptide-capped nanoparticles or peptide in solution was adjusted in the appropriate buffer (see below) in order to obtain an equivalent concentration of the functional peptide identical in each condition: 1.45 nM for Dot-blotting and 27 or 36 nM for Western-blotting.

For Western-blots,[37] peptide-capped nanoparticles were resuspended in loading buffer: Tris-HCl (75 mM, pH 6.8), SDS (6%, *w*/*v*), β-mercaptoethanol (3%, *v*/*v*), glycerol (18%, *v*/*v*) and Serva blue G (0.01%, *w*/*v*); and 5 μL were run on 18% SDS-Tris-Tricine gels as described previously by Schagger and von Jagow.[41] Note that in the loading buffer conditions, peptides are stripped off the nanoparticles and, therefore, migrate independently from the nanoparticles through the gel. After electrophoresis, gels were rinsed in transfer buffer and the peptides were then electro-transferred onto a silver- or gold-coated PVDF membrane (see below) using a semi-dry system (Multiphor II NovaBlot; Amersham Pharmacia Biotech). For Dot-blotting, peptide-capped gold nanoparticles in PBS (5 μL)

were blotted to PVDF membranes. For both the Dot-blot and Western-blot procedure, membranes were blocked by incubation for 40 min at room temperature in PBS containing BSA (5 mg mL^{-1}). Afterwards, the membranes were incubated for 40 min, at room temperature, in PBST-BSA (PBS supplemented with Tween 20 (0.5%, *v/v*, PBST) and 5 mg mL^{-1} of BSA) with Strep-Tactin-HRP (1:7500). Finally, the blots were washed with PBST (5×, 5 min) and rinsed with water before visualization using enhanced chemiluminescence (SuperSignal West Dura Substrate).

Preparation of silver- or gold-coated PVDF membranes: Silver nanoparticles (S-NPs, around 7 nm diameter) were prepared as follow: $AgNO_3$ (200 mL, 1 mM) was heated to near boiling in a water bath, sodium citrate (20 mL, 19.4 mM) was then added to the $AgNO_3$ and the mixture was heated for 10 min under mild agitation, at which time it was removed from the water bath and placed on a magnetic stirrer for an additional 15 min of agitation. Gold nanoparticles (5 nm) were purchased from BBI. PVDF membranes were wetted with ethanol (70%, *v/v*), rinsed with water and incubated for 40 min under agitation in the nanoparticle solution. Nanoparticle-coated membranes were then washed twice for 5 min with milliQ water and twice with the transfer buffer; transfer buffer: Tris(40 mM), Tricine (40 mM), SDS (0.04%, *w/v*), and methanol (20% *v/v*). See ref. [37] for further details.

Mass spectrometry: Following thrombin treatment, the cleaved material were analyzed by using a Waters MS Technologies Q-Tof Micro Mass spectrometer coupled to a LC Packings Ultimate nano HPLC system. The column used was a LC Packings PepMap C18 nano HPLC column. The solvent system was: 2% acetonitrile with 0.1% formic acid (solvent A), 80% acetonitrile with 0.1% formic acid (solvent B). The gradient was 5–100% solvent B in 50 min with a flow rate of 200 nL min^{-1}. The mass spectrometer was operated in the positive ion nano-electrospray mode and mass spectra were recorded over the mass range 80–2000 Da.

Molecular dynamics calculations: All molecular dynamics (MD) calculations were performed using the AMBER9 suite of programs[42] in conjunction with the generalized Amber.[43] The solvent environment was represented using the Generalised Born solvation model developed by Case and co-workers,[44] which has been shown to provide structural information that is in good agreement with explicit solvent models, even for highly charged systems.[45] This method has the advantage that conformational transitions are accelerated relative to simulations performed in explicit water due to a lack of solvent damping allowing for a highly efficient exploration of conformational space whilst maintaining the accuracy of the calculations.[46] MD simulations were run at 300 K with a salt concentration of 150 mM and used a cut-off of 25 Å. Partial charges for the non-standard biotinylated and BS3-modified amino acids were generated within the Antechamber module in AMBER9 using the AM1 Hamiltonian and the BCC charge fitting procedure.[47,48] The functional peptides and the matrix peptides were constructed and arranged on the surface using the LEAP module of AMBER. Our initial simulations were performed for a spherical surface constructed from 734 matrix peptides separated by approximately 8 Å in each direction. The N-terminal cysteine residues were held in place using restraints of 10 Kcal mol Å^{-2}. The system was firstly energy minimized and then slowly heated to 300 K. We then performed 1 ns of MD at 300 K using 64 processors of the 404 Opteron Myrinet supercomputer cluster available at Leeds. These preliminary simulations were used to measure the average height of the matrix peptide C-terminal asparagine above the surface of the gold nanoparticle, which we found to be approximately 12 Å. These preliminary simulations showed that the interaction of the functional peptides with the surface is dominated by electrostatic interactions between the negatively charged C-terminal of the asparagine on the matrix peptides and positively charged lysine and arginine residues. Therefore, to decrease the computational cost of subsequent calculations, we constructed a pair of 11 by 11 surfaces in which the CALNN matrix peptides are 8 Å apart and represented only by the C-terminal asparagine with an N-terminal acetyl group. These are held in position throughout the MD runs by restraints of 10 Kcal mol Å^{-2}. Two separate functional peptides were placed in the centre of each array, but now with their attachment points held so that their restrained N-termini are positioned ca. 12 Å above the C termini of the surface residues, as shown in Figure S6. The surface is given a curvature appropriate for a 5 nm radius gold particle decorated with peptides which are effectively 12 Å in length. We then performed simulated annealing MD simulations on 32 processors of the Leeds parallel supercomputer. The surface and the peptides were initially subjected to 1 ns MD at 300 K. This was followed by a 500 ps run at 500 K. The peptides were then re-equilibrated at 300 K for 500 ps prior to the next 500 ps data production phase. This heating–equilibration-data production procedure was repeated for 24 cycles of annealing for functional peptides with and without the BS3 linker. The vectors connecting the N-terminal cysteine sulfur atom and the side-chain nitrogen atom of Lys20 (in the absence of the BS3 linker) or on the reactive ester carbon atom of the BS3 were extracted from these MD trajectories. To quantify the spatial volume explored by each of the two functional peptides, we used these vectors to calculate the distribution of vertical and horizontal displacements of these key atoms from their attachment points on the surface. Electrostatic potential maps were calculated using the MM/PBSA functionality in AMBER9 at a salt concentration of 150 mM using a grid spacing of 0.5 Å, with internal and external dielectric constants of 4 and 80, respectively. Molecular graphics images were produced using the UCSF Chimera package from the Resource for Biocomputing, Visualization, and Informatics at the University of California, San Francisco (supported by NIH P41 RR-01081),[49] animations were produced using the VMD package.[50]

Statistical analysis: All calculations were performed by using MathCad.

Acknowledgements

This work was supported by the Biotechnology and Biological Sciences Research Council (BBSRC), the Cancer and Polio Research Fund, the Human Frontiers Science Programme and the North West Cancer Research Fund. S.H.H. thanks the UK National Grid Service for computing time. R.L. thanks BBSRC for a David Phillips Fellowship and Mathias Brust for critical reading of the manuscript.

Keywords: gold · nanoparticles · peptides · self-assembly · self-organization

[1] G. M. Whitesides, J. P. Mathias, C. T. Seto, *Science* **1991**, *254*, 1312.
[2] H. Cölfen, S. Mann, *Angew. Chem.* **2003**, *115*, 2452; *Angew. Chem. Int. Ed.* **2003**, *42*, 2350.
[3] R. P. Goodman, I. A. T. Schaap, C. F. Tardin, C. M. Erben, R. M. Berry, C. F. Schmidt, A. J. Turberfield, *Science* **2005**, *310*, 1661.
[4] J. H. Chen, N. C. Seeman, *Nature* **1991**, *350*, 631.
[5] G. E. Davies, G. R. Stark, *Proc. Natl. Acad. Sci. USA* **1970**, *66*, 651.
[6] S. J. L. Billinge, I. Levin, *Science* **2007**, *316*, 561.

[7] J. C. Love, L. A. Estroff, J. K. Kriebel, R. G. Nuzzo, G. M. Whitesides, *Chem. Rev.* **2005**, *105*, 1103.
[8] R. Lévy, *ChemBioChem* **2006**, *7*, 1141.
[9] A. K. Boal, V. M. Rotello, *J. Am. Chem. Soc.* **1999**, *121*, 4914.
[10] L. Pasquato, P. Pengo, P. Scrimin, *Supramol. Chem.* **2005**, *17*, 163.
[11] C. C. You, M. De, V. M. Rotello, *Curr. Opin. Chem. Biol.* **2005**, *9*, 639.
[12] K. Tamada, M. Hara, H. Sasabe, W. Knoll, *Langmuir* **1997**, *13*, 1558.
[13] S. J. Stranick, A. N. Parikh, Y. T. Tao, D. L. Allara, P. S. Weiss, *J. Phys. Chem.* **1994**, *98*, 7636.
[14] H. A. Behanna, K. Rajangam, S. I. Stupp, *J. Am. Chem. Soc.* **2007**, *129*, 321.
[15] H. M. McConnell, *Annu. Rev. Phys. Chem.* **1991**, *42*, 171.
[16] S. M. K. Davidson, S. L. Regen, *Chem. Rev.* **1997**, *97*, 1269.
[17] G. A. DeVries, M. Brunnbauer, Y. Hu, A. M. Jackson, B. Long, B. T. Neltner, O. Uzun, B. H. Wunsch, F. Stellacci, *Science* **2007**, *315*, 358.
[18] A. M. Jackson, J. W. Myerson, F. Stellacci, *Nat. Mater.* **2004**, *3*, 330.
[19] Chechik, Bjørnholm, Kondo, Schiffrin, Pasquato, Banin, Brust, Vanmaekelbergh, Uosaki, Horrocks, Yonezawa, Higgins, Calvo, Pileni, Landman, Liz-Marzán, Schmickler, Amiens, Zitoun, Davies, Murray, Benfield, Becker, Dryfe, *Faraday Discuss.* **2004**, *125*, 293.
[20] K. Nørgaard, M. J. Weygand, K. Kjaer, M. Brust, T. Bjørnholm, *Faraday Discuss.* **2004**, *125*, 221.
[21] C. Vilain, F. Goettmann, A. Moores, P. Le Floch, C. Sanchez, *J. Mater. Chem.* **2007**, *17*, 3509.
[22] P. R. Ghosh, A. Verma, V. M. Rotello, *Chem. Commun. (Cambridge, UK)* **2007**, 2796.
[23] Z. Y. Tang, Z. L. Zhang, Y. Wang, S. C. Glotzer, N. A. Kotov, *Science* **2006**, *314*, 274.
[24] M. C. Rechtsman, F. H. Stillinger, S. Torquato, *Phys. Rev. Lett.* **2005**, *95*.
[25] Z. L. Zhang, S. C. Glotzer, *Nano Lett.* **2004**, *4*, 1407.
[26] J. P. K. Doye, A. A. Louis, I.-C. Lin, L. R. Allen, E. G. Noya, A. W. Wilber, H. C. Kok, R. Lyus, *Phys. Chem. Chem. Phys.* **2007**, *9*, 2197.
[27] R. Levy, N. T. K. Thanh, R. C. Doty, I. Hussain, R. J. Nichols, D. J. Schiffrin, M. Brust, D. G. Fernig, *J. Am. Chem. Soc.* **2004**, *126*, 10076.
[28] M. Brust, D. Bethell, D. J. Schiffrin, C. J. Kiely, *Adv. Mater.* **1995**, *7*, 795.
[29] R. Elghanian, J. J. Storhoff, R. C. Mucic, R. L. Letsinger, C. A. Mirkin, *Science* **1997**, *277*, 1078.
[30] R. Lévy, Z. X. Wang, L. Duchesne, R. C. Doty, A. I. Cooper, M. Brust, D. G. Fernig, *ChemBioChem* **2006**, *7*, 592.
[31] A. G. Kanaras, Z. X. Wang, A. D. Bates, R. Cosstick, M. Brust, *Angew. Chem.* **2003**, *115*, 201; *Angew. Chem. Int. Ed.* **2003**, *42*, 191.
[32] S. R. Nicewarner Peña, S. Raina, G. P. Goodrich, N. V. Fedoroff, C. D. Keating, *J. Am. Chem. Soc.* **2002**, *124*, 7314.
[33] Z. X. Wang, R. Levy, D. G. Fernig, M. Brust, *J. Am. Chem. Soc.* **2006**, *128*, 2214.
[34] C. C. You, R. R. Arvizo, V. M. Rotello, *Chem. Commun. (Cambridge, UK)* **2006**, 2905.
[35] C. S. Yun, G. A. Khitrov, D. E. Vergona, N. O. Reich, G. F. Strouse, *J. Am. Chem. Soc.* **2002**, *124*, 7644.
[36] Some decrease at high Nav in column 4 of Figure 2C could be expected due to cross-linking between the Lys20 of two different functional peptides followed by cleavage. No decrease is observed indicating that accessibility of the enzyme to the cleavage site is reduced after cross-linking, and/or that Lys20 may preferentially cross-link Lys7 (on another chain).
[37] L. Duchesne, D. G. Fernig, *Anal. Biochem.* **2007**, *362*, 287.
[38] Removal of the excess peptide through centrifugations or centrifugal filtration takes several minutes; for this reason, the experiment was carried out in the presence of the excess peptide. It is therefore possible that excess peptide in solution but interacting with the monolayer through electrostatic interactions may contribute to the trimers and tetramers bands that can be seen in Figure 6. However, overinterpretation of these higher molecular-weight bands should be avoided because the gel and transfer conditions used in this study are optimized for the low molecular weights (monomers and dimers), and the results for the trimers and tetramers are therefore not as quantitative.
[39] A. J. Lomant, G. Fairbanks, *J. Mol. Biol.* **1976**, *104*, 243.
[40] G. Mattson, E. Conklin, S. Desai, G. Nielander, M. D. Savage, S. Morgensen, *Mol. Biol. Rep.* **1993**, *17*, 167.
[41] H. Schagger, G. Vonjagow, *Anal. Biochem.* **1987**, *166*, 368.
[42] D. A. Case, T. A. Darden, T. E. Cheatham, C. L. Simmerling, J. Wang, R. E. Duke, R. Luo, K. M. Merz, D. A. Pearlman, M. Crowley, R. C. Walker, W. Zhang, B. Wang, S. Hayik, A. Roitberg, G. Seabra, K. F. Wong, F. Paesani, X. Wu, S. Brozell, V. Tsui, H. Gohlke, L. Yang, C. Tan, J. Mongan, V. Hornak, G. Cui, P. Beroza, D. H. Mathews, C. Schafmeister, W. S. Ross, P. A. Kollman, *AMBER Biomolecular Simulation Progreams*, University of California, San Francisco, **2006**.
[43] J. M. Wang, R. M. Wolf, J. W. Caldwell, P. A. Kollman, D. A. Case, *J. Comput. Chem.* **2004**, *25*, 1157.
[44] V. Tsui, D. A. Case, *Biopolymers* **2000**, *56*, 275.
[45] Z. A. Sands, C. A. Laughton, *J. Phys. Chem. B* **2004**, *108*, 10113.
[46] S. A. Harris, C. A. Laughton, T. B. Liverpool, *Nucleic Acids Res.* **2008**, *36*, 21–29.
[47] A. Jakalian, B. L. Bush, D. B. Jack, C. I. Bayly, *J. Comput. Chem.* **2000**, *21*, 132.
[48] A. Jakalian, D. B. Jack, C. I. Bayly, *J. Comput. Chem.* **2002**, *23*, 1623.
[49] E. F. Pettersen, T. D. Goddard, C. C. Huang, G. S. Couch, D. M. Greenblatt, E. C. Meng, T. E. Ferrin, *J. Comput. Chem.* **2004**, *25*, 1605.
[50] W. Humphrey, A. Dalke, K. Schulten, *J. Mol. Graphics* **1996**, *14*, 33.

Received: May 13, 2008
Published online on August 12, 2008

